This journal is © The Royal Society of Chemistry 2023

Facile synthesis approach of bifunctional Co-Ni-Fe oxyhydroxide and spinel oxide composite electrocatalysts from hydroxide and layered double hydroxide composite precursor

Shoo Kitano, Yuki Sato, Reiko Tagsari, Ruijie Zhu, Damian Kowalski, Yoshitaka Aoki, Hiroki Hamasaki**

*Sho Kitano: Division of Applied Chemistry, Faculty of Engineering, Hokkaido University, Sapporo, Hokkaido 060-8628, Japan

Yuki Sato: Graduate School of Chemical Sciences and Engineering, Hokkaido University, Sapporo, Hokkaido 060-8628, Japan

Reiko Tag sari: Graduate School of Chemical Sciences and Engineering, Hokkaido University, Sapporo, Hokkaido 060-8628, Japan

Ruijie Zhu: Graduate School of Chemical Sciences and Engineering, Hokkaido University, Sapporo, Hokkaido 060-8628, Japan

Damian Kowalski: Biological and Chemical Research Centre (CNBC), Faculty of Chemistry, University of Warsaw, up. Zikri i Wigury 101, 02-089, Warsaw, Poland

Yoshitaka Aoki: Division of Applied Chemistry, Faculty of Engineering, Hokkaido University, Sapporo, Hokkaido 060-8628, Japan

*Hiroki Hamasaki: Division of Applied Chemistry, Faculty of Engineering, Hokkaido University, Sapporo, Hokkaido 060-8628, Japan

Table S1 Metal composition ratio of the reaction solution and prepared catalysts measured by SEM-EDX.

Solution (at.%)			Catalyst (at.%)		
Co	Ni	Fe	Co	Ni	Fe
85	5	10	72	6	22
78	15	7	65	20	15
88	10	2	84	12	4
90	5	5	80	6	14
85	10	5	74	13	13
95	-	5	94	-	6
95	5	-	80	20	-

Table S2 Metal composition ratio of the prepared catalysts measured by ICP-AES.

Catalyst (at.%)		
Co	Ni	Fe
69	6	25
63	21	16
83	12	5
78	7	15
73	13	14
89	-	11
79	21	-

Table S3 Activity comparison of several bifunctional electrocatalysts.

Catalyst	$E_{1/2}$ (V vs RHE)	$E_{di=10}$ (V vs RHE)	ΔE (V)	Ref.
$Co_{74}Ni_{13}Fe_{13}$ (150)	0.87	1.51	0.64	This work
$MnFe_2O_4/NiCo_2O_4$	0.83	1.56	0.73	[1]
Mn_3O_4@$CoMn_2O_4$-CoxOy	0.83	1.68	0.85	[2]
$CuCoO_x$/FeOOH	0.78	1.5	0.72	[3]
Pd@PdO-Co_3O_4	0.75	1.56	0.81	[4]
$MnO_2/La_{0.7}Sr_{0.3}MnO_3$	0.76	1.82	1.06	[5]
Co_3O_4@NiFe LDHs	0.77	1.55	0.78	[6]
MnO@Co–N/C	0.83	1.76	0.93	[7]
nNiFe LDH/3D MPC	0.86	1.57	0.71	[8]
MnVOx@N–rGO	0.80	1.65	0.85	[9]
FeCoOOH-NS/NF 3D-FeNC	0.855	1.46	0.605	[10]
$Mn_{0.5}(Fe_{0.3}Ni_{0.7})_{0.5}$Ox/MWCNTs-Ox	0.84	1.57	0.73	[11]
$NiCo_2O_4$/Co,N–CNTs NCs	0.862	1.569	0.707	[12]

Table S4 Activity and durability comparison of several air-electrodes.

Catalyst	$E_{1/2}$ (V vs RHE)	$E_{j=10}$ (V vs RHE)	ΔE (V)	Durability (h(cycle))	Current density	Ref.
$Co_{74}Ni_{13}Fe_{13}$ (150)	0.76	1.48	0.72	550 (260)	20	This work
Ca_2FeCoO_5	0.62	1.51	0.89	200 (100)	20	[13]
$NiCo_2O_4$ @FeNi LDH	-0.18 (vs Hg/HgO)	0.43 (vs Hg/HgO)	0.61	20(20)	20	[14]
$MnCo_2O_4$	0.91	1.57	0.66	20(10)	20	[15]
$NiFeO@MnO_x$	0.805	1.593	0.788	20(300)	5(OER), 3(ORR)	[16]

Table S5 The ratio of metals dissolved in the electrolyte to the total amount of catalyst during the durability cycle test.

Dissolution (at.%)		
Co	Ni	Fe
0.032	0.11	0.21

Table S6 Performance comparison of the $Co_{74}Ni_{13}Fe_{13}$ (150) and state-of-the-art catalysts.

Catalyst	Open circuit potential (V)	Power density (mW cm^{-2})	Durability (h (cycle))	Current density (mA cm^{-2})	Ref.
$Co_{74}Ni_{13}Fe_{13}$ (150)	-	195	430 (1290)	10	This work
NP-Co_3O_4/CC	1.58	200	400	5	[17]
CeO_2/Co_3O_4@NC	1.41	117	(350)	5	[18]
$(FeCoNi)_3O_4$/Mn_3O_4	1.44	136	400 (2400)	2	[19]
Ni|MnO/CNF	1.59	139	120 (350)	10	[20]
Co_9S_8/CNT	1.3	200	96 (576)	10	[21]
FeCo-DHO/NCNTs	1.4	193	300 (1800)	5	[22]
CoNi@NCNT/NF	1.4	127	90	5	[23]
P–Co_3O_4 NWs	1.42	72.1	500 (500)	2	[24]
CoO/Co_xP	1.4	123	200 (400)	5	[25]
Co@Co_3O_4@NC-900	-	64	200 (100)	5	[26]
FeCo@MNC	1.4	115	24 (144)	20	[27]
Co_2FeO_4/NCNTs	1.43	91	100 (600)	50	[28]

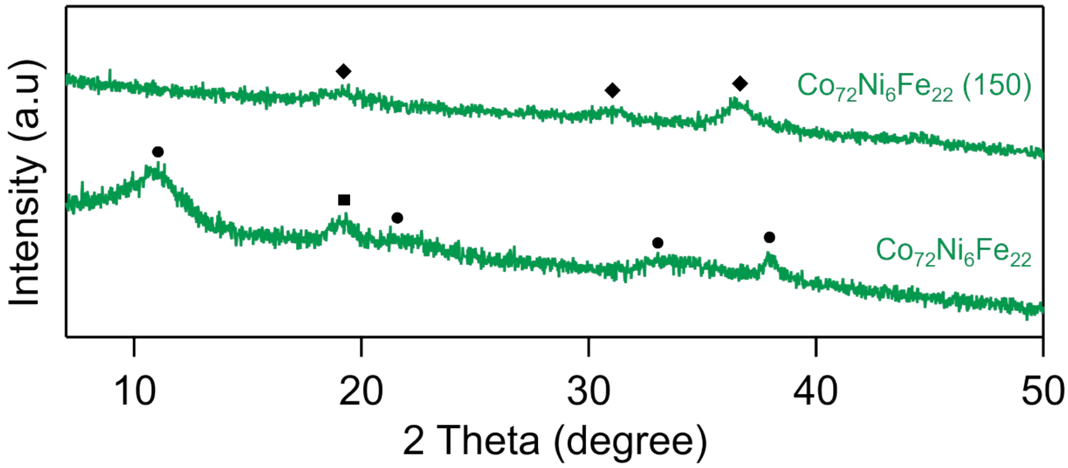

Figure S1. XRD patterns of the $Co_{72}Ni_6Fe_{22}$ and $Co_{72}Ni_6Fe_{22}$(150) (circle: LDH, square: hydroxide, diamond: spinel oxide).

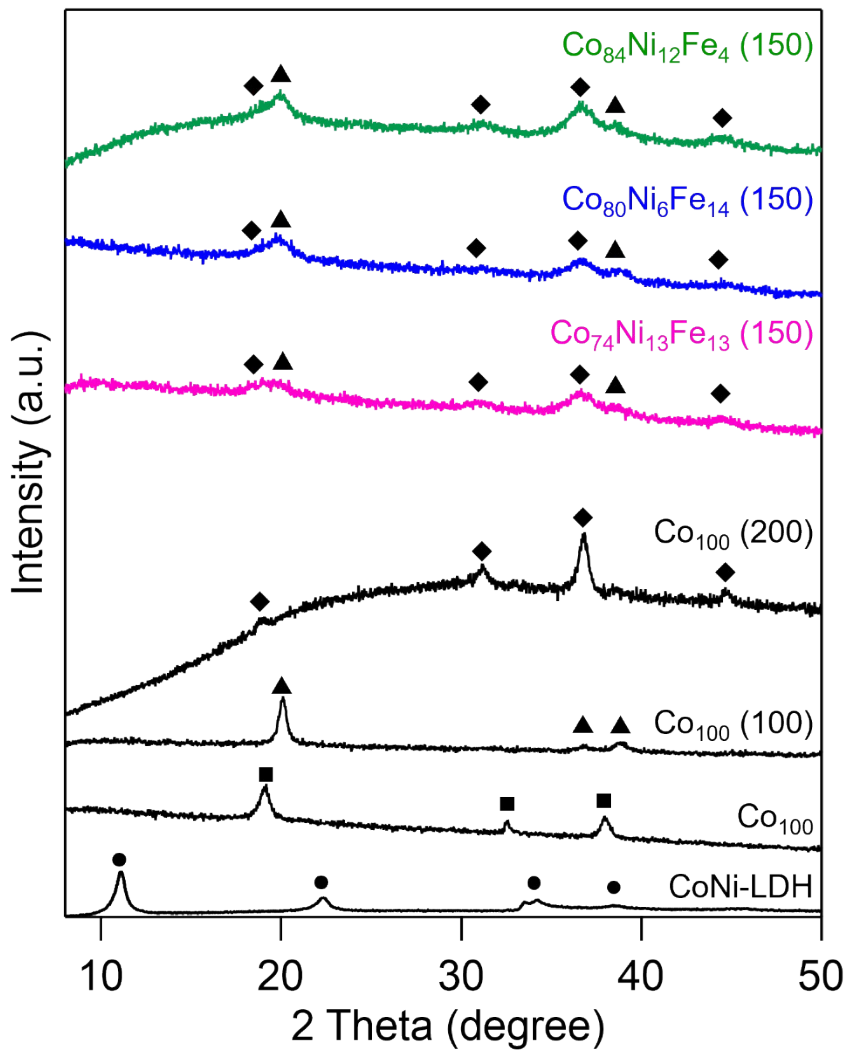

Figure S2. XRD patterns of the composite catalysts calcined at 150°C, Co_{100}, corresponding calcined Co_{100} samples and CoNi-LDH reference (circle: LDH, square: hydroxide, triangle: oxyhydroxide, diamond: spinel oxide).

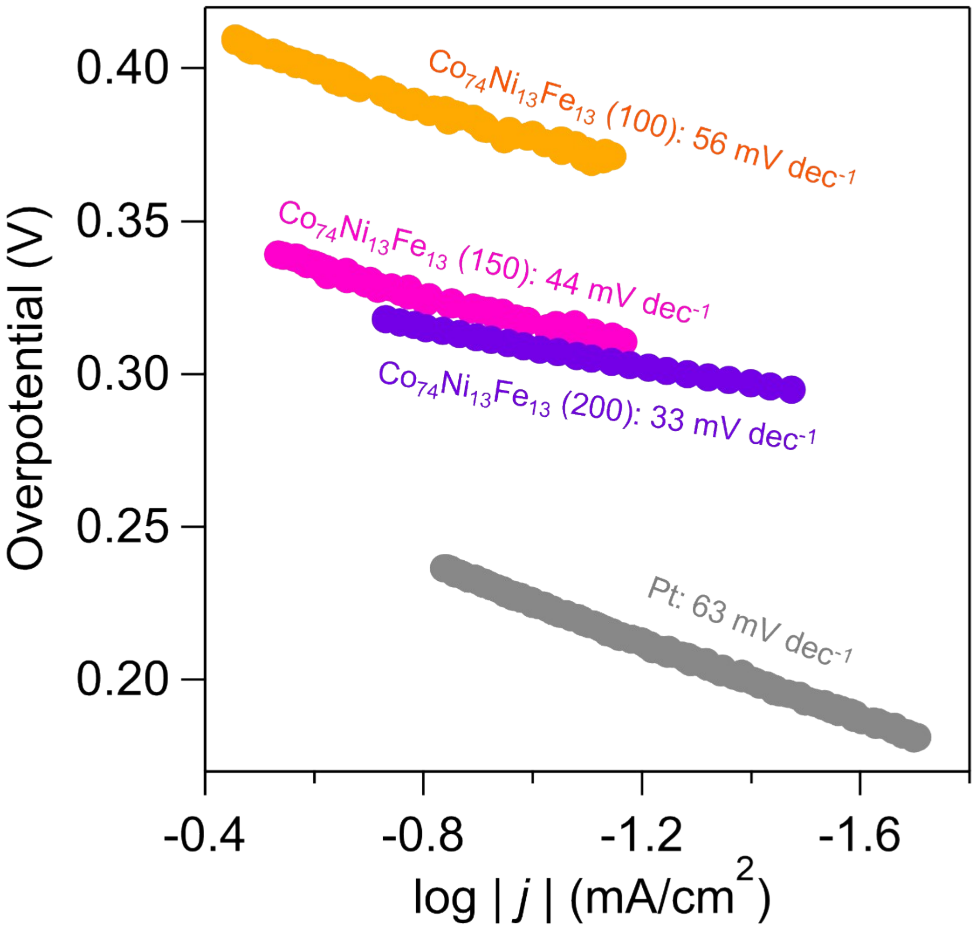

Figure S3. Tafel slopes of the $Co_{74}Ni_{13}Fe_{13}$ (T) catalysts and Pt/C for ORR in an O_2-saturated 4 mol dm^{-3} KOH solution.

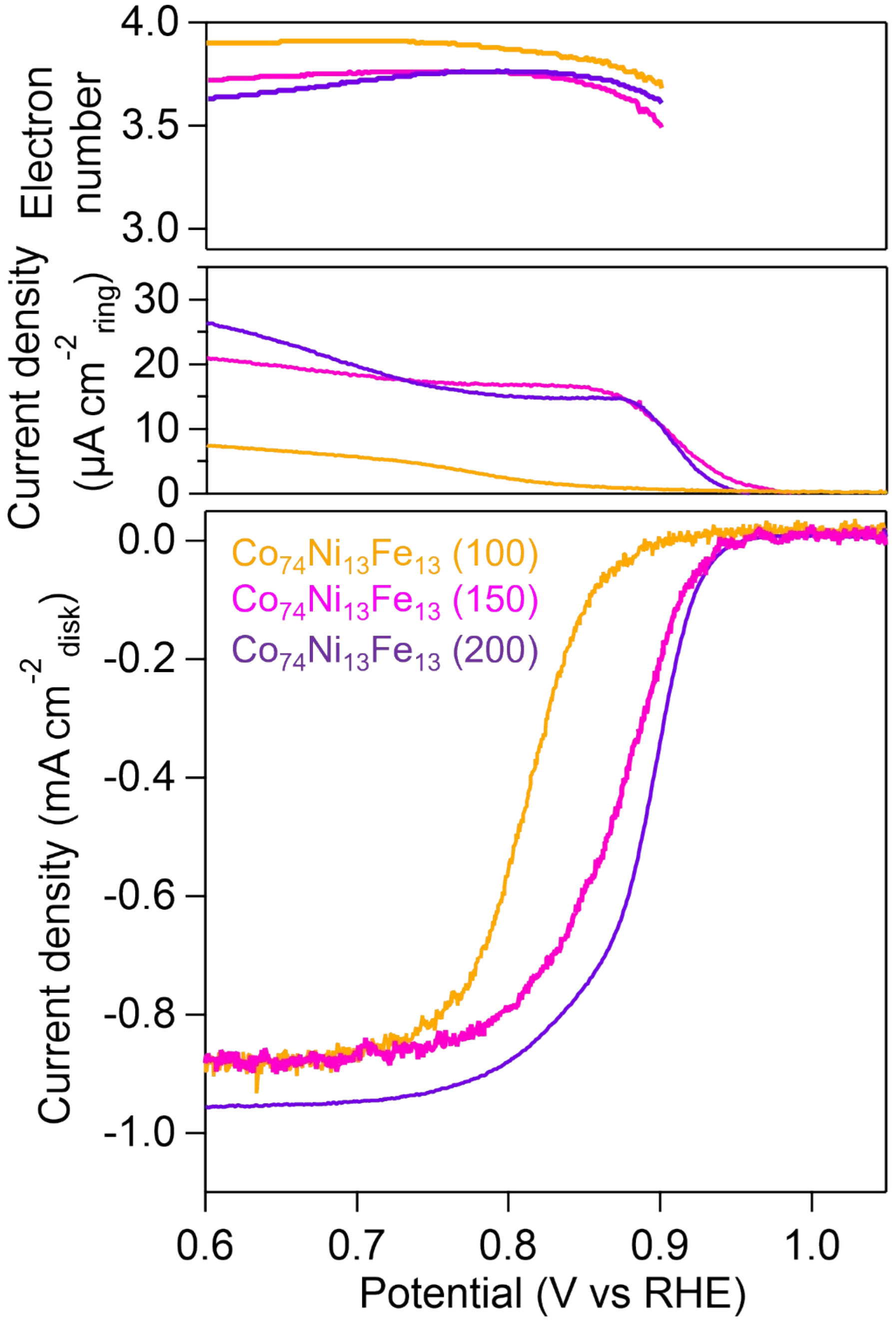

Figure S4. Disk current, ring current and electron number of the $Co_{74}Ni_{13}Fe_{13}$ (T) catalysts for ORR in an O_2-saturated 4 mol dm^{-3} KOH solution.

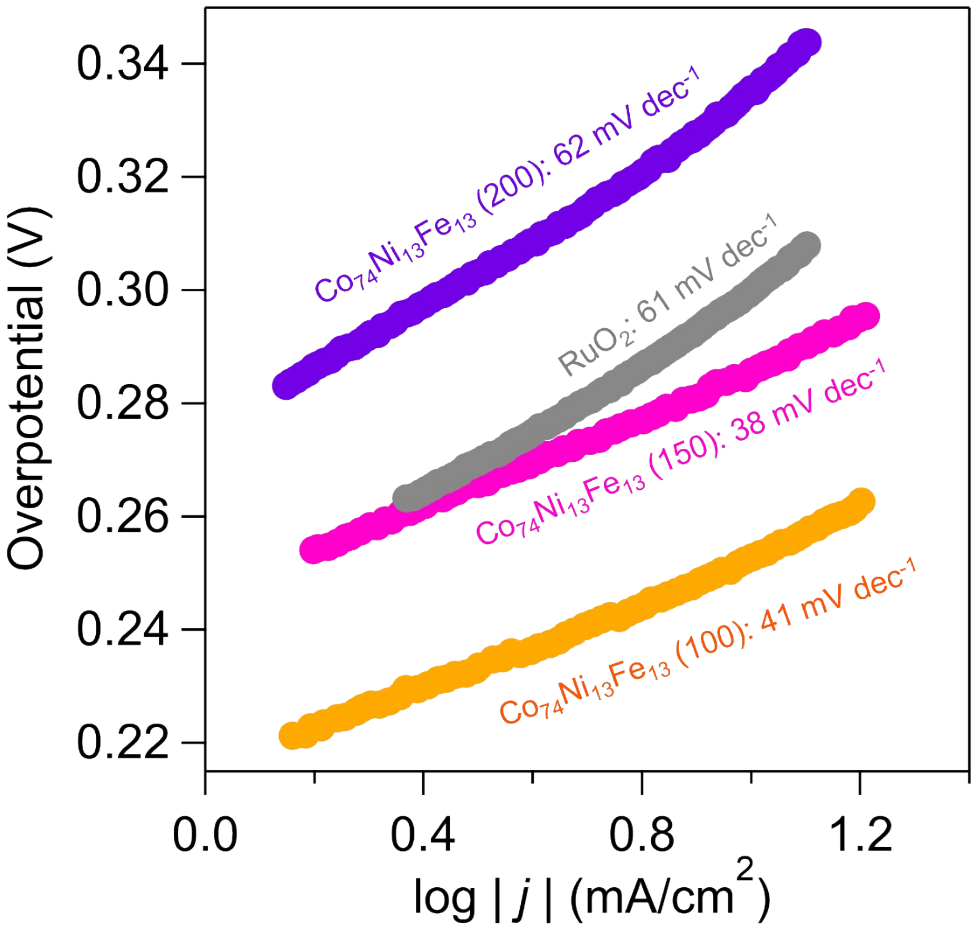

Figure S5. Tafel slopes of the $Co_{74}Ni_{13}Fe_{13}$ (T) catalysts and RuO_2 for OER in O_2-saturated 4 mol dm^{-3} KOH solution.

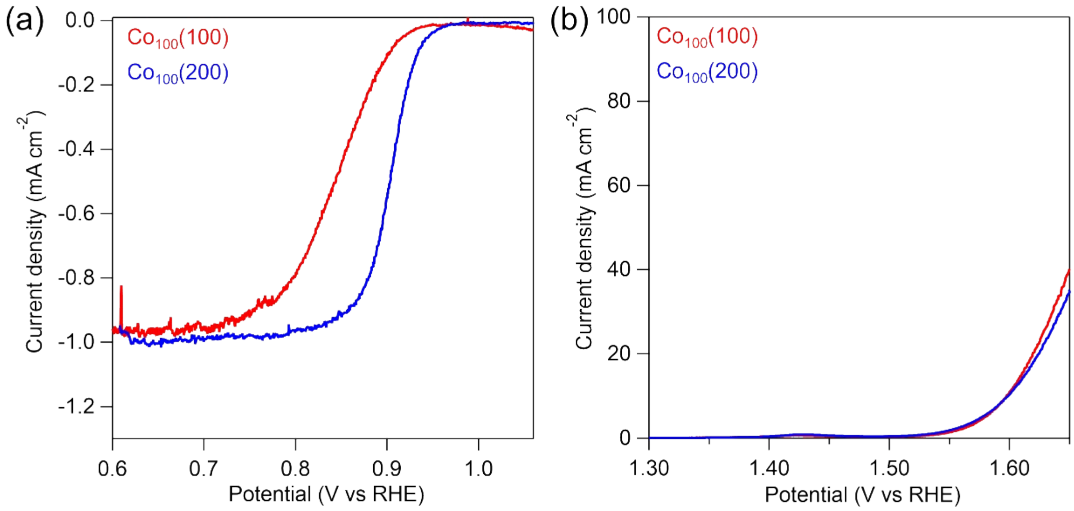

Figure S6. Polarization curves of the Co_{100}(150) and Co_{100}(200) for (a) ORR and (b) OER in O_2-saturated 4 mol dm^{-3} KOH solution.

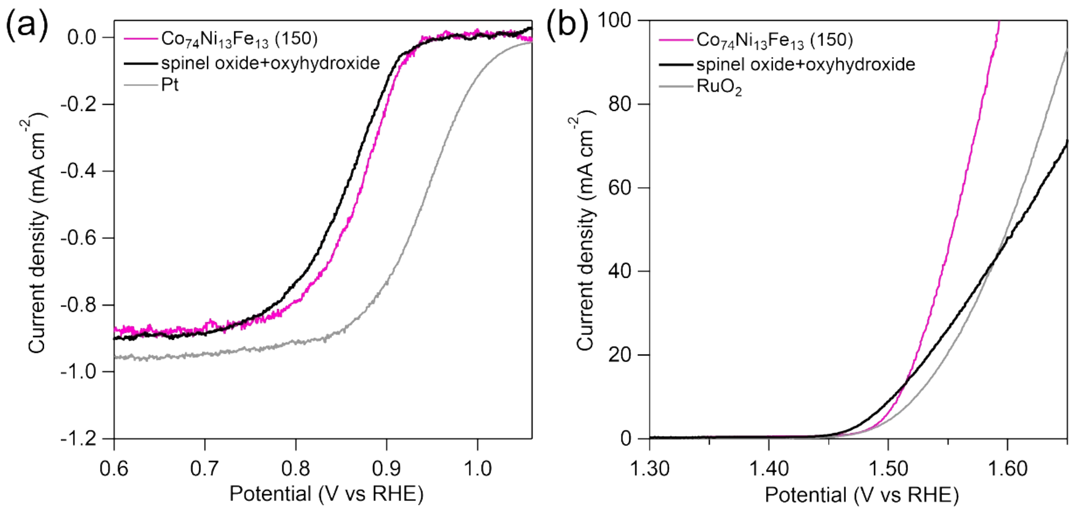

Figure S7. Polarization curves of the $Co_{74}Ni_{13}Fe_{13}$(150), physically mixed sample, Pt and RuO_2 for (a) ORR and (b) OER in O_2-saturated 4 mol dm^{-3} KOH solution. The physically mixed sample was prepared by mixing equal amounts of the $Co_{74}Ni_{13}Fe_{13}$(100) and $Co_{74}Ni_{13}Fe_{13}$(200) using an agate mortar.

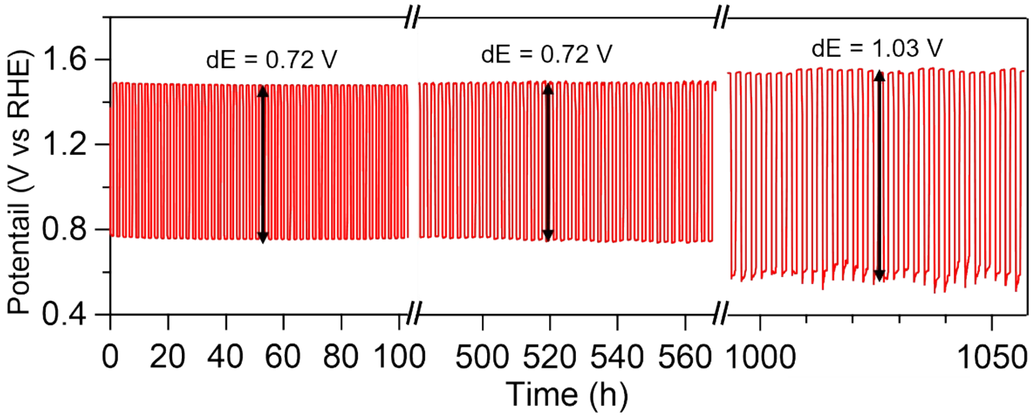

Figure S8. Charge-discharge cycle performance of the $Co_{74}Ni_{13}Fe_{13}$(150) air-electrode at 20 mA cm^{-2} in 4 mol dm^{-3} KOH aqueous solution.

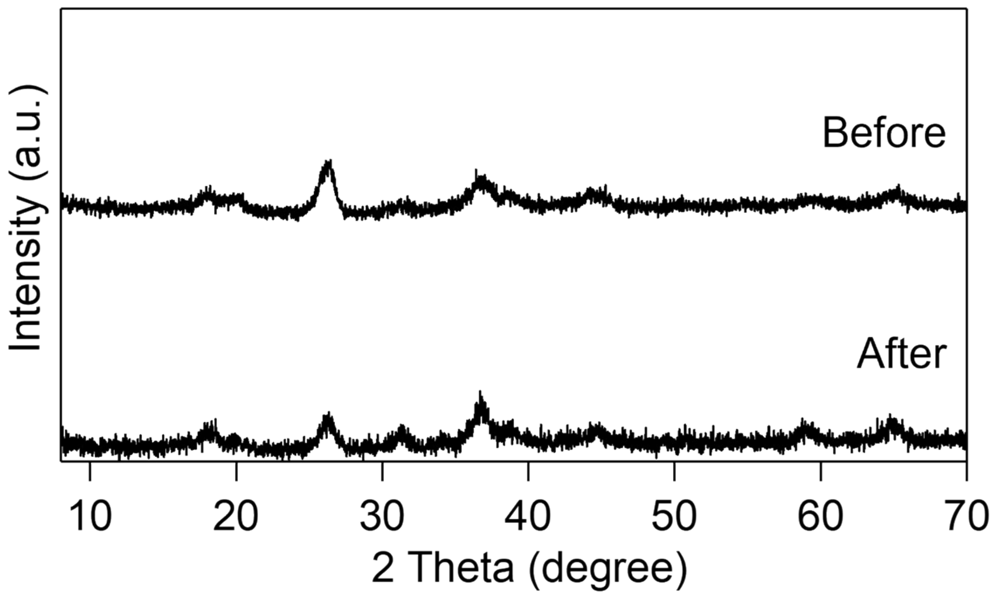

Figure S9. XRD patterns of the $Co_{74}Ni_{13}Fe_{13}$ (150) air-electrode before and after cycle test.

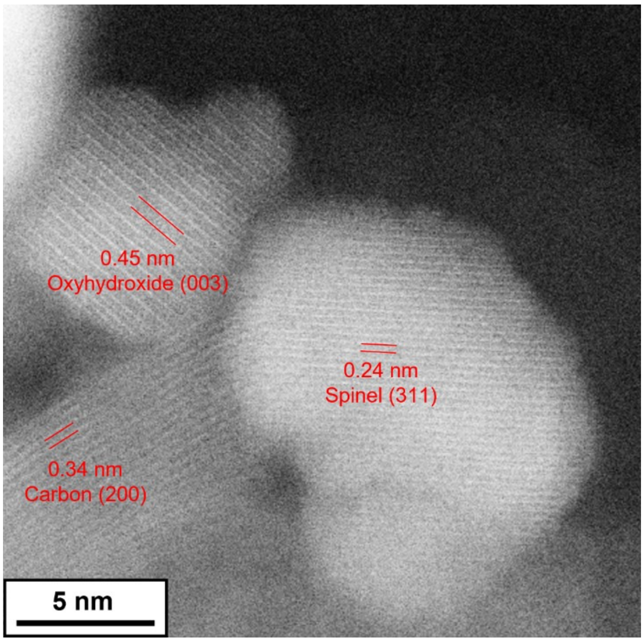

Figure S10. HAADF-STEM image of the catalyst layer of air-electrode after cycle test.

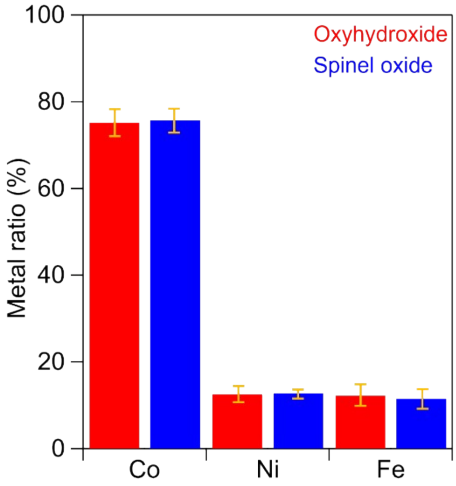

Figure S11. Metal composition ratio of oxyhydroxide and spinel oxide constituting the $Co_{74}Ni_{13}Fe_{13}$ (150) catalyst after the cycle test.

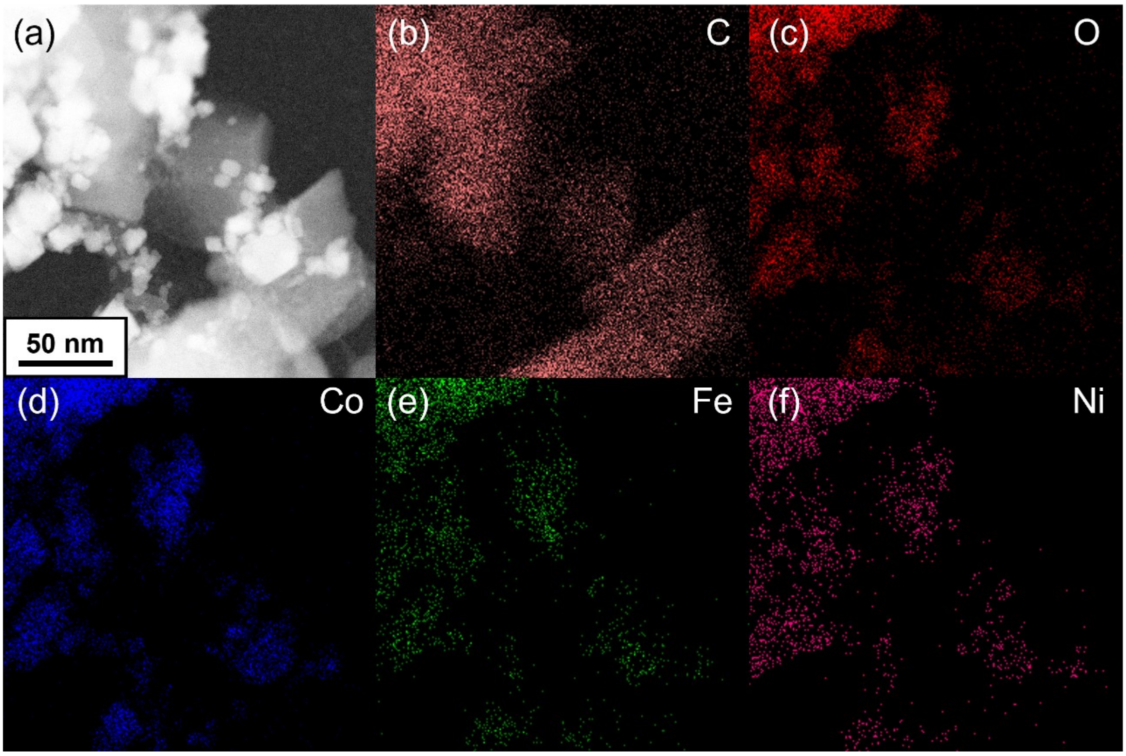

Figure S12. (a) HAADF-STEM image and STEM-EDX maps for (b) C-K, (c) O-K, (d) Co-K, (e) Fe-K and (f) Ni-K of the catalyst layer of air-electrode after the cycle test.

References

1. Y. Q. Zhang, M. Li, B. Hua, Y. Wang, Y. F. Sun and J. L. Luo, *Appl Catal B-Environ*, 2018, **236**, 413-419.
2. Z. S. Luo, E. Irtem, M. Ibanez, R. Nafria, S. Marti-Sanchez, A. Genc, M. de la Mata, Y. Liu, D. Cadavid, J. Llorca, J. Arbiol, T. Andreu, J. R. Morante and A. Cabot, *Acs Appl Mater Inter*, 2016, **8**, 17435-17444.
3. M. Kuang, Q. H. Wang, H. T. Ge, P. Han, Z. X. Gu, A. M. Al-Enizi and G. F. Zheng, *Acs Energy Lett*, 2017, **2**, 2498-2505.
4. H. C. Li, Y. J. Zhang, X. Hu, W. J. Liu, J. J. Chen and H. Q. Yu, *Adv Energy Mater*, 2018, **8**.
5. S. S. Yan, Y. J. Xue, S. H. Li, G. J. Shao and Z. P. Liu, *Acs Appl Mater Inter*, 2019, **11**, 25870-25881.
6. X. L. Guo, X. L. Hu, D. Wu, C. Jing, W. Liu, Z. L. Ren, Q. N. Zhao, X. P. Jiang, C. H. Xu, Y. X. Zhang and N. Hu, *Acs Appl Mater Inter*, 2019, **11**, 21506-21514.
7. Y. N. Chen, Y. B. Guo, H. J. Cui, Z. J. Xie, X. Zhang, J. P. Wei and Z. Zhou, *J Mater Chem A*, 2018, **6**, 9716-9722.
8. W. Wang, Y. C. Liu, J. Li, J. Luo, L. Fu and S. L. Chen, *J Mater Chem A*, 2018, **6**, 14299-14306.
9. X. L. Xing, R. J. Liu, K. C. Cao, U. Kaiser, G. J. Zhang and C. Streb, *Acs Appl Mater Inter*, 2018, **10**, 44511-44517.
10. S. Ibraheem, S. G. Chen, J. Li, Q. M. Wang and Z. D. Wei, *J Mater Chem A*, 2019, **7**, 9497-9502.
11. D. M. Morales, M. A. Kazakova, S. Dieckhofer, A. G. Selyutin, G. V. Golubtsov, W. Schuhmann and J. Masa, *Adv Funct Mater*, 2020, **30**.
12. J. Li, S. Q. Lu, H. L. Huang, D. H. Liu, Z. B. Zhuang and C. L. Zhong, *Acs Sustain Chem Eng*, 2018, **6**, 10021-+.
13. E. Tsuji, T. Motohashi, H. Noda, D. Kowalski, Y. Aoki, H. Tanida, J. Niikura, Y. Koyama, M. Mori, H. Arai, T. Ioroi, N. Fujiwara, Y. Uchimoto, Z. Ogumi and H. Habazaki, *Chemsuschem*, 2017, **10**, 2864-2868.
14. L. Wan, Z. H. Zhao, X. X. Chen, P. F. Liu, P. C. Wang, Z. Xu, Y. Q. Lin and B. G. Wang, *Acs Sustain Chem Eng*, 2020, **8**, 11079-11087.
15. Y. Sato, S. Kitano, D. Kowalski, Y. Aoki, N. Fujiwara, T. Ioroi and H. Habazaki, *Electrochemistry*, 2020, **88**, 566-573.
16. Y. Cheng, S. Dou, M. Saunders, J. Zhang, J. Pan, S. Y. Wang and S. P. Jiang, *J Mater Chem A*, 2016, **4**, 13881-13889.
17. X. Wang, Z. Q. Liao, Y. B. Fu, C. Neumann, A. Turchanin, G. Nam, E. Zschech, J. Cho, J. Zhang and X. L. Feng, *Energy Storage Mater*, 2020, **26**, 157-164.
18. X. B. He, X. R. Yi, F. X. Yin, B. H. Chen, G. R. Li and H. Q. Yin, *J Mater Chem A*, 2019, **7**, 6753-6765.

19. S. Y. Li, X. Y. Zhou, G. Fang, G. Q. Xie, X. J. Liu, X. Lin and H. J. Qiu, *Acs Appl Energ Mater*, 2020, **3**, 7710-7718.

20. D. X. Ji, J. G. Sun, L. D. Tian, A. Chinnappan, T. R. Zhang, W. A. D. M. Jayathilaka, R. Gosh, C. Baskar, Q. Y. Zhang and S. Ramakrishna, *Adv Funct Mater*, 2020, **30**.

21. H. Li, Z. Guo and X. W. Wang, *J Mater Chem A*, 2017, **5**, 21353-21361.

22. M. J. Wu, Q. L. Wei, G. X. Zhang, J. L. Qiao, M. X. Wu, J. H. Zhang, Q. J. Gong and S. H. Sun, *Adv Energy Mater*, 2018, **8**.

23. W. H. Niu, S. Pakhira, K. Marcus, Z. Li, J. L. Mendoza-Cortes and Y. Yang, *Adv Energy Mater*, 2018, **8**.

24. B. S. Tang, J. Yang, Z. K. Kou, L. Xu, H. L. Seng, Y. N. Xie, A. D. Handoko, X. X. Liu, Z. W. Seh, H. Kawai, H. Gong and W. F. Yang, *Energy Storage Mater*, 2019, **23**, 1-7.

25. Y. Niu, M. L. Xiao, J. B. Zhu, T. T. Zeng, J. D. Li, W. Y. Zhang, D. Su, A. P. Yu and Z. W. Chen, *J Mater Chem A*, 2020, **8**, 9177-9184.

26. Z. Y. Guo, F. M. Wang, Y. Xia, J. L. Li, A. G. Tamirat, Y. R. Liu, L. Wang, Y. G. Wang and Y. Y. Xia, *J Mater Chem A*, 2018, **6**, 1443-1453.

27. C. L. Li, M. C. Wu and R. Liu, *Appl Catal B-Environ*, 2019, **244**, 150-158.

28. X. T. Wang, T. Ouyang, L. Wang, J. H. Zhong, T. Y. Ma and Z. Q. Liu, *Angew Chem Int Edit*, 2019, **58**, 13291-13296.